

Classification of Hand Flexion/Extension Using High-density ECoG

Tianxiao Jiang, Tao Jiang, Taylor Wang, Shenshen Mei, Qingzhu Liu, Yunlin Li,
Xiaofei Wang, Sujit Prabhu, Zhiyi Sha, Nuri F. Ince*

*Department of Biomedical Engineering,
University of Houston, Houston, Texas, USA 77204-5060
Email: nfince@uh.edu

Abstract—Grasping is one of the most important hand movements performed in daily life and therefore a hand neuroprosthetic should be able to achieve this function with high accuracy. Electroencephalogram (ECoG) recorded from standard clinical electrodes has been proposed as a potential control signal in brain-machine interfaces (BMIs) and used to provide information about executed motor activity such as arm movement direction and individual finger movements. Here, we investigate the value of ECoG recorded from human motor cortex with high density electrodes to distinguish between hand flexion and extension in single trial level for a hand neuroprosthetic. Two subjects were asked to execute spontaneous hand extension and flexion during the recording. Event-related desynchronization (ERD) and event-related synchronization (ERS) in low-frequency band (LFB: 8-32 Hz) and high-frequency band (HFB: 60-200 Hz) were observed in both subjects during these executed movements. ECoG signal was bandpass filtered in three subbands, alpha (8-13 Hz), beta (13-32 Hz) and gamma (60-200 Hz) for classification. A common spatial pattern (CSP) algorithm fused with linear discriminant analysis (LDA) was used to distinguish between executed movements. In both subjects, the gamma band yielded classification accuracies close to 100%. Alpha and beta bands provided poor classification results with higher latency compared to gamma band. These results suggested that the gamma band spatial patterns of motor cortex captured with high-density ECoG can effectively distinguish between hand extension and flexion. High-density ECoG can be a promising modality to drive a neural prosthetic which can help paralyzed patients to regain crucial daily hand functions.

Keywords—High-density ECoG; Time-frequency map; CSP; LDA.

I. INTRODUCTION

ECoG was initially performed in clinical setting to determine the extent of resection in epilepsy cases intraoperatively [1][2]. Nowadays, ECoG is used not only for clinical decision making but also in BMI studies to establish the communication and control function. Compared to scalp electroencephalogram (EEG), the ECoG provides higher signal quality and wider bandwidth as it is recorded directly from the cortex.

Previous studies have found that sensorimotor activity is correlated with the power changes in specific subbands of ECoG [3]. Amplitude modulations in gamma band (40-200 Hz) were found to be closely related to motor behaviors. In the past few years, features extracted from the gamma range of ECoG or local field potentials have been extensively used to decode hand movements of both human and non-human primates [4]–[6]. Previous ECoG based BMI studies generally use large clinical grids with an inter-electrode spacing of 10 mm. With the advancements in micro electrode technology today, the spatial resolution of ECoG has dramatically increased. Recent studies have just started to show the potential of high-density

ECoG in decoding human motor functions including cursor control [7], differentiation between multiple hand gestures [5] and to drive a prosthetic limb online [8].

In this study we explored the spatial patterns of ECoG recorded from two subjects during hand flexion and extension tasks. In particular, a customized high-density grid with 120 channels (12×10, 1.2 mm contact exposure and 4 mm spacing) was used to assess cortical activity with superior resolution compared to clinical electrodes with 10mm contact spacing. We characterized the time-frequency dynamics and investigated to what extend the recorded activity can be used to distinguish between hand extension and flexion to drive a neuroprosthetic. In detail, we studied the contribution of ECoG subbands to the classification of the executed tasks. Moreover, rather than focusing on grasping only, we focused on the differentiation between hand flexion and extension to improve the functions of a hand prosthetic and aimed to answer the question whether these activities are associated with different patterns in ECoG.

II. MATERIALS AND METHODS

Below we describe the experimental setup and signal processing techniques used in this study.

A. Experimental setup

A customized 120 (12×10) channel high-density electrode grid with a contact diameter of 1.2 mm and inter-electrode distance of 4 mm was used in this study. The electrodes were placed on the cortex of two subjects who require functional mapping and monitoring during awake brain surgery. The ECoG were intraoperatively recorded along with forearm EMG and bipolar ECG (lead-II) for 15-20 mins period with a 2 kHz sampling frequency and 16 bit A/D resolution. During the recordings, the subjects were asked to perform hand extension/flexion according to auditory instructions. Each movement type was executed for 30 times and followed by 2-3 seconds resting period. Hand movements and the finger positions were digitized by a digital glove. The finger position data provided by the digital glove are further synchronized with the ECoG via simultaneously recorded trigger signal. The details of the system setup were described in [9].

B. Time-frequency maps

ECoG data were manually scrutinized to exclude bad channels. A series of FIR notch filters were applied to suppress 50 Hz power line noise and its harmonics up to 200 Hz. The movement onsets were annotated according to the changes in finger positions and EMG data. The ECoG data were aligned with respect to movement onset and each trial consisted three seconds of data centered at movement onset (1.5s before and

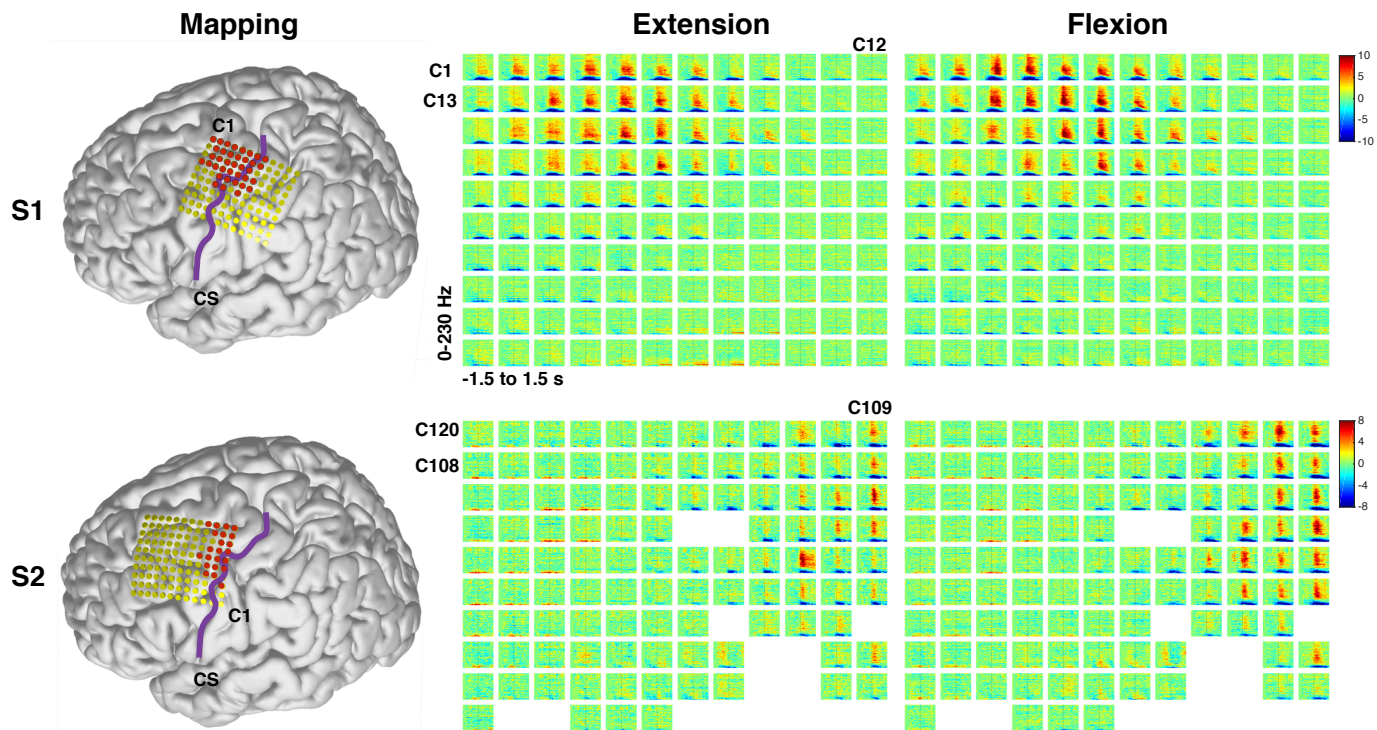


Figure 1. Electrode locations are shown on a 3D rendering of a template brain surface (left). Contacts with clear power increase (ERS) in the high gamma band during movements are marked as red. The central sulcus (CS) is highlighted by a purple line. Each time-frequency map is from -1.5 to 1.5 s, with movement onset at zero second, and covers 0-230 Hz. All maps are displayed in dB scale (S1: -10 to 10, S2: -8 to 8).

1.5s after). After eliminating those segments with artifacts, 25 trials of flexion and 22 trials of extension in total were available for S1. For S2, the total number of trials were 26 and 20 for flexion and extension respectively. Using available trials for each task, an averaged time-frequency map of each channel was computed using short-time Fourier transform (STFT) with 256-sample long Hanning window. The window was shifted with 90% overlap at each step. After computing the averaged time-frequency maps for each channel in hand movement, they were normalized by the average spectrum of the first 500 ms (S_B):

$$S_N = 10 \times \log_{10} \frac{S_A}{S_B} \quad (1)$$

The normalized time-frequency maps were used to inspect the power changes in peri-movement period in different frequency bands. Identified bands were used to quantify the amount of ERD and ERS in each. In this study, ERD was computed in LFB (8-32 Hz) and ERS was computed in HFB (60-200 Hz) based on our observation from time-frequency analysis.

C. Classification

In order to distinguish between the executed tasks, a CSP algorithm was used to extract the spatial patterns of ECoG. CSP is designed to search for an optimal spatial projection that maximizes the variance ratio of projected data between two conditions [10]. Originally implemented in EEG studies to capture the movement related subband power change (LFB-ERD), CSP has been successfully extended to ECoG studies as ERD and ERS were consistently observed in ECoG recordings.

Although both alpha (8-13 Hz) and beta (13-32 Hz) in LFB were associated with ERD, they were usually separately studied as different information conveyed within each subband. In this study, three subbands, alpha (8-13 Hz), beta (13-32 Hz) and gamma (60-200 Hz), were tested for classification. After filtering the data in each subband, averaged spatial covariance matrix was computed for each movement. The optimization problem of CSP can be transformed to the equivalent generalized eigenvalue problem [11]:

$$\Sigma^0 w = \lambda \Sigma^1 w \quad (2)$$

where, w is the generalized eigenvector and λ is the generalized eigenvalue. Σ^0 denotes the averaged covariance of flexion while Σ^1 denotes extension. The variance (energy) ratio between flexion and extension is equivalent to λ here. After obtaining the eigenvalue spectrum, usually a few eigenvectors related to the top and bottom of the spectrum were used for feature extraction [11]. In order to avoid overfitting, we only used two projections, one related to the largest eigenvalue and the other related to the smallest eigenvalue. The two dimensional feature extracted by these two projections was used in LDA for classification. Classification error rates were estimated at each time point using 800 ms of data before that time point. 5×5 cross-validations were performed to generalize the classification accuracies. At each cross validation, the training subset was used to compute the averaged covariance matrices (Σ^0 and Σ^1). In more detail, at each trial, the covariance matrix was computed based on the multi-channel data of 800 ms at specific time point. For each movement, the obtained covariance matrices were averaged across all trials

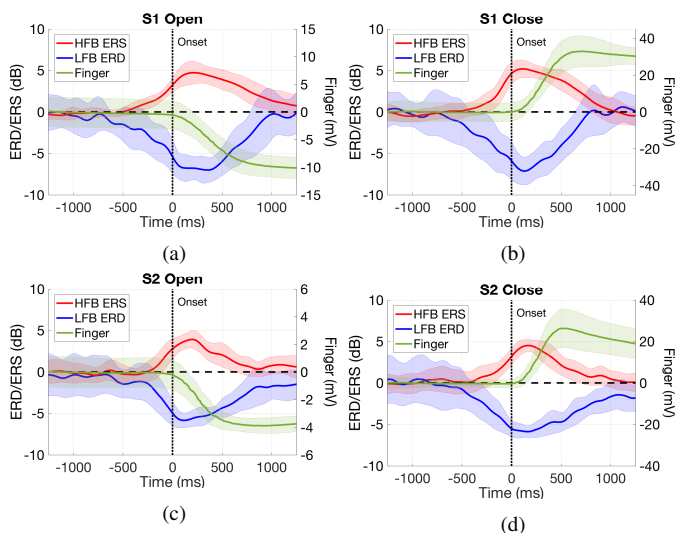


Figure 2. Average ERD (blue) and ERS (red) and average finger positions (green). LFB: 8-32 Hz. HFB: 60-200 Hz. Shaded regions denote the standard deviations across trials.

to yield Σ^0 and Σ^1 . After solving Equation 2, the resulting linear projections were used in conjunction with LDA for classification on the test set.

III. RESULTS

The signal analysis and classification results of this study are provided in this section. Specifically, the time frequency analysis of each channel, ERD/ERS analysis and finally the classification results are presented in detail.

A. Time-frequency maps of ECoG grid

The electrode grid was registered onto a template brain surface by comparing the landmarks (central sulcus, midline) of the individual MRI and intraoperative photographs (Figure 1). The normalized time-frequency maps of all channels are displayed on the right side of Figure 1. Although there existed differences between individuals in terms of the level of spectral modulations, for both subjects, we observed clear power decrease in LFB (8-32 Hz) and increase in HFB (60-200 Hz) from sensorimotor areas. ERS in HFB was observed to be more spatially localized while ERD in LFB was more widespread.

B. Event related power changes

ERD in LFB and ERS in HFB from selected channels were averaged and displayed from 1.5 seconds before movement onset to 1.5 seconds after it (Figure 2). Averaged finger positions were also provided in each hand flexion and extension (Figure 2, green). The shaded regions represent the standard deviations across all trials. ERD were observed to have smaller magnitude than ERS in terms of absolute value. Generally, both ERD and ERS happened slightly before the movement onset.

C. Classification

The classification results obtained from three subbands are provided in Figure 3. For both subjects, gamma band

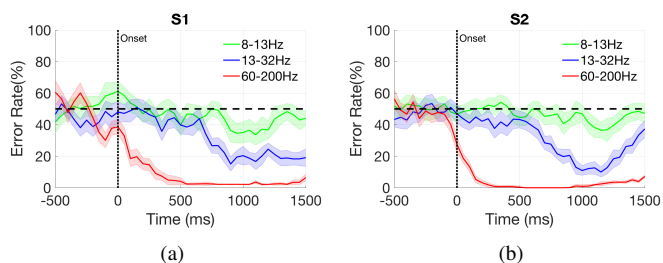


Figure 3. The classification error rates using three different sub-bands: alpha (8-13 Hz, green), beta (13-32 Hz, blue) and high gamma (60-200 Hz, red) in S1 (a) and S2 (b).

consistently yielded better classification results compared to alpha and beta bands. Specifically, in S1, the classification error rate of gamma band at movement onset was 38.54% while alpha and beta band only provided chance level (50%) decoding accuracy. The minimum error rate (2.31%) in S1 was obtained by gamma band at around 500 ms. Both alpha and beta band achieved their maximum classification accuracies at around 1000 ms. However, beta band yielded better classification accuracy compared to alpha band. For S2, the classification error rate at movement onset of gamma band was 27.56% which is clearly better than alpha and beta. Gamma band achieved zero classification error rate at 500 ms. At 250 ms, gamma band already yielded an error rate of 1.82%. Alpha and beta bands reached their best decoding at around 1200 ms. Similar to S1, beta band outperformed alpha band in terms of minimum classification error rate (9.96% versus 36.44%).

IV. DISCUSSION

Neural prosthetics based on ECoG in future can potentially improve the quality of life of paralyzed patients by helping them regain crucial daily hand functions. To our knowledge, for the first time, this study demonstrated the use of ECoG data recorded from a high-density grid to distinguish hand flexion and extension movements of human subjects for a neuroprosthetics. In particular, a high-density ECoG electrode grid (12×10) with 1.2 mm contact size and 4mm spacing was used in this study to investigate cortical activity of hand flexion and extension at very fine temporal and spatial resolution. We decoded the ECoG signal by using the CSP algorithm and LDA to distinguish between executed movements. The decoding system achieved 98-100% discrimination accuracy between hand flexion and extension using the gamma band (60-200 Hz). The classification accuracies in the alpha (8-13 Hz) and beta (13-32 Hz) band were poor and lagged the movement onset dramatically. These results indicated that the gamma band signal from high-density ECoG can be effectively used to differentiate between hand flexion and extension.

Through visual inspection of the time-frequency maps of all channels (Figure 1), ERD in LFB presents similar widespread spatial extent between two tasks while ERS in gamma band is spatially localized and distinct between hand flexion and extension. The most activated ERS channels differ slightly between movements. In addition to the differences in spatial extent, ERS during flexion is also stronger in terms of magnitude compared to extension. The spatial differences together with magnitude differences between movements in gamma band might be utilized by the CSP algorithm to form

an optimal spatial projection that can effectively distinguish between hand flexion and extension.

The best classification accuracies were achieved between 250- 500 ms following the movement onset in both subjects. Since the CSP features are computed in a 800ms window, this might suggest that data from both motor planning phase and execution period contribute to the decoding accuracy. However, as CSP in this study utilized all channels, sensory feedback from those channels located on the sensory cortex might also contribute to the classification results after movement onset. In future studies, CSP needs to be restricted to motor cortex to exclude sensory feedback. We also noticed that ERS in gamma band generally lasts for a few hundred milliseconds (Figure 2) following the movement onset and was stronger during the initiation of the movement but not during the maintenance.

Although the study was executed in two subjects only, we observed that the gamma band consistently yielded almost perfect classification accuracies. Consistently in both subjects, the low band was associated with poor classification accuracies and larger latency. Given the consistent results obtained from both subjects, in the future, our decoding technique based on high-density ECoG can be extended to real-time online decoding applications to establish a hand neural prosthetic.

ACKNOWLEDGMENT

We appreciate the cooperations of our subjects and valuable support of Haidian Hospital in this study.

REFERENCES

- [1] W. Penfield and H. Jasper, *Epilepsy and the functional anatomy of the brain*. Boston: Little Brown, 1954.
- [2] A. Palmieri, "The concept of the epileptogenic zone: a modern look at Penfield and Jasper's views on the role of interictal spikes." *Epileptic disorders : international epilepsy journal with videotape*, vol. 8 Suppl 2, aug 2006, pp. S10-5. [Online]. Available: <http://www.ncbi.nlm.nih.gov/pubmed/17012068>
- [3] K. J. Miller, M. DenNijs, P. Shenoy, J. W. Miller, R. P. N. Rao, and J. G. Ojemann, "Real-time functional brain mapping using electrocorticography," *NeuroImage*, vol. 37, 2007, pp. 504-507.
- [4] N. F. Ince, R. Gupta, S. Arica, A. H. Tewfik, J. Ashe, and G. Pellizzer, "High accuracy decoding of movement target direction in non-human primates based on common spatial patterns of local field potentials." *PLoS one*, vol. 5, no. 12, jan 2010, p. e14384. [Online]. Available: <http://journals.plos.org/plosone/article?id=10.1371/journal.pone.0014384>
- [5] M. G. Bleichner, Z. V. Freudenburg, J. M. Jansma, E. J. Aarnoutse, M. J. Vansteensel, and N. F. Ramsey, "Give me a sign: decoding four complex hand gestures based on high-density ECoG." *Brain structure & function*, oct 2014. [Online]. Available: <http://www.ncbi.nlm.nih.gov/pubmed/25273279>
- [6] Y. Nakanishi, T. Yanagisawa, D. Shin, C. Chen, H. Kambara, N. Yoshimura, R. Fukuma, H. Kishima, M. Hirata, and Y. Koike, "Decoding fingertip trajectory from electrocorticographic signals in humans." *Neuroscience research*, vol. 85, aug 2014, pp. 20-7. [Online]. Available: <http://www.ncbi.nlm.nih.gov/pubmed/24880133>
- [7] W. Wang, J. L. Collinger, A. D. Degenhart, E. C. Tyler-Kabara, A. B. Schwartz, D. W. Moran, D. J. Weber, B. Wodlinger, R. K. Vinjamuri, R. C. Ashmore, J. W. Kelly, and M. L. Boninger, "An electrocorticographic brain interface in an individual with tetraplegia." *PLoS one*, vol. 8, no. 2, jan 2013, p. e55344. [Online]. Available: <http://journals.plos.org/plosone/article?id=10.1371/journal.pone.0055344>
- [8] G. Hotson, D. P. McMullen, M. S. Fifer, M. S. Johannes, K. D. Katyal, M. P. Para, R. Armiger, W. S. Anderson, N. V. Thakor, B. A. Wester, and N. E. Crone, "Individual finger control of a modular prosthetic limb using high-density electrocorticography in a human subject," *Journal of Neural Engineering*, vol. 13, no. 2, 2016, p. 026017. [Online]. Available: <http://stacks.iop.org/1741-2552/13/i=2/a=026017?key=crossref.2d5ef8bc47143308a3a1ff00aabb53dd>
- [9] T. Jiang, N. F. Ince, T. Jiang, T. Wang, S. Mei, Y. Li, X. Wang, S. Prabhu, and Z. Sha, "Investigation of the spatial and spectral patterns of hand extension/flexion using high-density ECoG," in *7th International IEEE/EMBS Conference on Neural Engineering (NER)*. IEEE, apr 2015, pp. 589-592. [Online]. Available: <http://ieeexplore.ieee.org/lpdocs/epic03/wrapper.htm?arnumber=7146691>
- [10] H. Ramoser, J. Muller-Gerking, and G. Pfurtscheller, "Optimal spatial filtering of single trial EEG during imagined hand movement," *IEEE Transactions on Rehabilitation Engineering*, vol. 8, no. 4, 2000, pp. 441-446. [Online]. Available: <http://ieeexplore.ieee.org/lpdocs/epic03/wrapper.htm?arnumber=895946>
- [11] B. Blankertz, R. Tomioka, S. Lemm, M. Kawanabe, and K.-r. Muller, "Optimizing Spatial filters for Robust EEG Single-Trial Analysis," *IEEE Signal Processing Magazine*, vol. 25, no. 1, 2008, pp. 41-56. [Online]. Available: <http://ieeexplore.ieee.org/lpdocs/epic03/wrapper.htm?arnumber=4408441>